OXFORD

Cerebral Cortex, June 2021;31: 2812–2821

doi: 10.1093/cercor/bhaa389
Advance Access Publication Date: 12 January 2021
Original Article

ORIGINAL ARTICLE

Pubertal Testosterone and the Structure of the Cerebral Cortex in Young Men

Zhijie Liao[1], Yash Patel[2], Ammar Khairullah[3], Nadine Parker[2] and Tomas Paus[1,3]

[1]Department of Psychology, University of Toronto, Toronto, ON M5S3G3, Canada, [2]Institute of Medical Sciences, University of Toronto, Toronto, ON M5S3G3, Canada and [3]Department of Psychiatry, University of Toronto, Toronto, ON M5S3G3, Canada

Address correspondence to Tomas Paus, Department of Psychology, University of Toronto, 100 St. George Street, 4th Floor, Sidney Smith Hall, Toronto, ON M5S3G3, Canada. Email: tomas.paus@utoronto.ca.

Abstract

Adolescence is a period of brain maturation that may involve a second wave of organizational effects of sex steroids on the brain. Rodent studies suggest that, overall, organizational effects of gonadal steroid hormones decrease from the prenatal/perinatal period to adulthood. Here we used multimodal magnetic resonance imaging to investigate whether 1) testosterone exposure during adolescence (9–17 years) correlates with the structure of cerebral cortex in young men ($n = 216$, 19 years of age); 2) this relationship is modulated by the timing of testosterone surge during puberty. Our results showed that pubertal testosterone correlates with structural properties of the cerebral cortex, as captured by principal component analysis of T1 and T2 relaxation times, myelin water fraction, magnetization transfer ratio, fractional anisotropy and mean diffusivity. Many of the correlations between pubertal testosterone and the cortical structure were stronger in individuals with earlier (vs. later) testosterone surge. We also demonstrated that the strength of the relationship between pubertal testosterone and cortical structure across the cerebral cortex varies as a function of inter-regional profiles of gene expression specific to dendrites, axonal cytoskeleton, and myelin. This finding suggests that the cellular substrate underlying the relationships between pubertal testosterone and cerebral cortex involves both dendritic arbor and axon.

Key words: ALSPAC, axon, dendrite, testosterone surge, two-stage model

Introduction

Sex steroids shape brain structure and function (Pfaff and Joëls 2016). During development, long-lasting (permanent) changes induced by sex steroids are referred to as organizational effects. Although the perinatal period is thought to be a time of maximal sensitivity to such organizational effects of sex steroids (Phoenix et al. 1959), recent studies suggest that puberty represents yet another sensitive period in this regard (Sisk and Zehr 2005; Peper et al. 2011; Herting et al. 2014). Based on work in rodents (Sisk and Zehr 2005; Schulz and Sisk 2006), Schulz and colleagues proposed a two-stage model of postnatal development in which the perinatal period of steroid-dependent sexual differentiation is followed by a second wave of steroid-dependent neural organization during adolescence (Schulz, Molenda–Figueira, et al. 2009a). In particular, they also incorporated an extended-window model that shows decreasing sensitivity to organizational effects of gonadal steroid hormones from the perinatal period to adulthood (Schulz and Sisk 2016). In this model, the two stages of hormone-dependent neural organization coincide with the time when—in males—testosterone becomes elevated rather than being driven by the opening/closing of two discrete sensitive periods. This model is supported mostly by studies in testosterone-related behaviors of nonhuman animals, which found that the early testosterone treatments most effectively facilitated adult mating behavior (Eaton 1970; Coniglio and Clemens 1976; Schulz

and Sisk 2016). For example, prepubertal testosterone treatment in gonadectomized male hamsters had a greater impact on adult reproductive function than testosterone treatment during puberty (Schulz, Zehr, et al. 2009b).

A growing body of studies carried out with magnetic resonance imaging (MRI) in humans has provided evidence of testosterone-related variations in gray and white matter during adolescence (Peper et al. 2011). For example, in adolescence, testosterone correlates positively with the volume of white matter and negatively with the volume of gray matter and cortical thickness (Perrin et al. 2008; Neufang et al. 2009; Paus et al. 2010; Nguyen 2018). Some studies found, however, no or opposite relationships (Peper et al. 2009; Bramen et al. 2012). Inspired by evidence from rodent studies suggesting that there is a decreasing window of sensitivity to testosterone throughout adolescence (Schulz and Sisk 2016), it is possible that associations between testosterone and the maturing human brain could be modulated by the timing of testosterone surge during puberty. For example, one study found an age- and pubertal stage-related decrease in the strength of the relationship between testosterone and cortical thickness (Nguyen et al. 2013). But the critical time period for effects of pubertal testosterone on brain structure in humans and possible underlying mechanisms remain unknown.

Furthermore, the microstructural underpinnings of testosterone-related variations in brain macrostructure are still unknown. Using different MRI modalities, namely T1-weighted and magnetization transfer ratio (MTR), Perrin et al. speculated that testosterone-related increases in white matter volume during male adolescence may be related to changes in axon diameter rather than the thickness of the myelin sheath (Perrin et al. 2008); this hypothesis was subsequently confirmed in *in vivo* and *in vitro* experimental studies (Pesaresi et al. 2015). This study indicated an advantage of multimodal MRI in revealing possible mechanisms relating to testosterone and brain structure. Studies in experimental animals and cell-culture experiments provided evidence in support of the effects of testosterone on axon growth (Mack et al. 1995; Fargo et al. 2008); for instance, removal of endogenous testosterone by castration was associated with lower axon diameter (and a lower *g* ratio; *g* ratio = axon diameter/fiber diameter; where fiber diameter = axon diameter + myelin sheath) in castrated male rats than intact male rats (Pesaresi et al. 2015). We also know that, in rats and mice, testosterone and/or other androgen are able to induce dendritic spines (Leranth et al. 2003), dendritic growth (Goldstein et al. 1990), and myelination (Abi Ghanem et al. 2017). These studies indicate that testosterone-related variations in brain structure on a macroscale may involve modifications of dendrites, axon, and myelin.

In this study, we took advantage of a multimodal MRI dataset and longitudinal data on testosterone trajectories during puberty to investigate 1) the relationship between pubertal testosterone and structural properties of cerebral cortex in young men; and 2) modulation of this relationship by the timing of testosterone surge during puberty. If humans show declining sensitivity to organizational effects of testosterone at puberty, we predict that the relationship between pubertal testosterone and cerebral cortex would be stronger in individuals with an early onset of testosterone surge than those with a late-onset. Using a virtual histology approach that uses publicly available data of gene expression across the human cerebral cortex (Shin et al. 2018; Parker et al. 2020), we also explored the possible cellular substrate underlying the association between testosterone and brain structure. The MRI dataset includes quantitative T1 relaxation time (T1), T2 relaxation time (T2), myelin water fraction (MWF), fractional anisotropy (FA), mean diffusivity (MD), and MTR. Both T1 and T2 are sensitive to water content and myelin (Laule et al. 2007; Edwards et al. 2018). MWF, estimated as a ratio of short T2 and total T2 components, is an index of myelin density (Laule et al. 2008; O'Muircheartaigh et al. 2019). FA and MD reflect, respectively, directional (or anisotropic) motion and the average motion of water. MTR depends on the transfer of spins between free protons (in water) and bound protons (bound to macromolecules); it is believed to index macromolecules of myelin (Laule et al. 2007; Mancini et al. 2020) as well as those in the cellular membranes of neurites (Uematsu et al. 2004; Patel et al. 2019). Considering the complex cellular composition of cerebral cortex and debates on the connection between MRI metrics and microstructural features, using multimodal MRI may provide a chance to gain insights of the microstructural mechanism underlying the association between testosterone and cerebral cortex.

Materials and Methods

Participants

As specified in our previous publications (Khairullah et al. 2014; Patel et al. 2020), the sample of young men studied here was recruited from the Avon Longitudinal Study of Parents and Children (ALSPAC). This is a birth cohort that included pregnant women from Avon county, the United Kingdom, with an expected delivery date between 1 April 1991 to 31 December 1992. Subsequently, longitudinal data have been collected using self-administered questionnaires and clinical examinations carried out during study visits (Boyd et al. 2013; Fraser et al. 2013). Blood samples were taken at select visits over the course of the study, roughly at the following years of age: 7, 9, 11, 13, 15, and 17. Ethical approval for the study was obtained from the ALSPAC Law and Ethics Committee. Note that the study website contains details of all the data that are available through a fully searchable data dictionary and variable search tool (http://www.bristol.ac.uk/alspac/researchers/our-data/).

As part of the ALSPAC project, we recruited 507 male participants who were 18 years of age or over, and had at least three blood samples available for the assessment of testosterone levels just before and during their adolescence (any combination of three or more samples obtained at 9, 11, 13, 15, and 17 years of age). Details of the sampling method have been described in our previous reports (Khairullah et al. 2014; Jensen et al. 2018). To obtain accurate measurements of average levels of bioavailable testosterone throughout puberty, and the age of peak testosterone change, this report was restricted to participants who had blood collected at all five visits ($n = 232$). After performing quality control on MRI and testosterone data, 216 of these 232 participants with good quality MRI matrices (age $=19.10 \pm 0.73$) were included in this analysis. Details of quality control are described below.

Testosterone

To obtain the measurement of average levels of bioavailable testosterone throughout puberty, we assayed levels of testosterone and sex hormone binding globulin (SHBG) in plasma, and estimated its trajectory from 9 to 17 years for each participant. We then calculated a measure of average level of testosterone by dividing the area under the curve of the testosterone trajectory

by the number of months between the first and last blood sample. We used the equation from (Södergard et al. 1982) in conjunction with the SHBG concentrations, and adjusted values of total testosterone to derive the values of bioavailable testosterone (details in Khairullah et al. 2014). In the text below, we refer to this measure as "pubertal-T." To characterize the timing of testosterone surge, we calculated age at peak testosterone change (APTC) for each participant using testosterone measures collected at each of the five visits as described above. Briefly, the testosterone data and the age of each testosterone collection for each participant were fitted with a cubic spline. From the derivative of the testosterone by age curve, we ascertained the age (in months) when the peak of testosterone change occurred (details in Khairullah et al. 2014).

MRI Data Acquisition and Processing

MRI scans were acquired on a General Electric 3 T HDx scanner with the following sequences; multicomponent driven equilibrium single pulse observation of T1 and T2 (mcDESPOT; Deoni et al. 2008), MTR, DWI, and T1-weighted imaging. Details regarding the MR sequences have been described previously (Björnholm et al. 2017). In brief, mcDESPOT was acquired using a 3D fast spoiled gradient recall (SPGR), with 8 T1-weighted SPGR, 2 inversions prepared SPGR, and 15 T1/T2 weighted steady-state free precession images at a resolution of $1.72 \times 1.72 \times 1.70$ mm. The DWI acquisition included 30 gradient directions with $b = 1200$ s/mm^2, and 3 ($b = 0$ s/mm^2) nondiffusion weighted images with a resolution of 2.40 mm isotropic. MT imaging was acquired using a 3D SPGR scan with (MTon) and without (MToff) a magnetization radio-frequency off-resonance pulse of 2 kHz, with a resolution of 1.90 mm isotropic. T1-weighted images were acquired at 1 mm isotropic using an inversion recovery fast SPGR sequence.

T1w scans were processed through an automated cortical reconstruction pipeline by FreeSurfer v6.0.0 ("recon-all"). Imaging data acquired with mcDESPOT were preprocessed at Cardiff University Brain Research Imaging Centre; this involved fitting fast and slow relaxing water via the mcDESPOT model (Deoni et al. 2008). MTR was calculated as follows: (MToff—MTon)/MToff (Tofts 2003). DWI maps underwent 1) correction for eddy current distortion, 2) brain extraction, and 3) diffusion tensor imaging (DTI) model fitting using FSL's toolset "eddy_correct," "bet," and "dtifit," respectively (Jenkinson et al. 2012). Quantitative T1, T2, MWF, MTR, and the B0 DTI map were registered to native FreeSurfer space using 6-parameter linear registration followed by diffeomorphic intrasubject intermodality registration from Advanced Normalization Tools (Avants et al. 2009). This nonlinear diffeomorphic registration was also used to account for possible phase-encoding-related distortions in the DTI data. Maps of FA and MD were registered to native FreeSurfer space using the transforms from the B0 registration above. MRI derived measures were sampled in the middle of the cerebral cortex, that is, between the pial surface and gray-white matter boundary (Patel et al. 2020); these single-voxel measures were averaged within each of 34 cortical regions (left hemisphere) parcellated in the Desikan–Killiany atlas (Desikan et al. 2006). Since the gene expression values used in our analysis were restricted to the left hemisphere, we used the brain measurements from 34 regions of the left hemisphere. Note that we observed strong correlations between the left and right inter-regional profiles in all six MRI modalities (MWF: $r = 0.872$; T1: $r = 0.963$; T2: $r = 0.906$; FA: $r = 0.956$; MD: $r = 0.907$; MTR: $r = 0.947$). Statistical outliers were defined as ± 3SD.

A total of 216 participants (with five blood samples) completed all scanning using the same MRI protocol. Six participants, who completed the full protocol with a different DWI sequence or failed to pass quality control of the image-analysis pipeline, were excluded from this study. Quality control was based on successful registration of MR scans to T1w, and completion of cortical reconstruction by FreeSurfer without any reported errors.

Principal Component Analysis of the Six MRI Modalities

Most of the six modalities correlated with each other to some extent (Supplementary Figure S1) but we make no specific assumptions about common (latent) factors operating across the modalities. Therefore, rather than using factor analysis, we applied principal component analysis (PCA) to describe common variance across the six modalities, and thus reduce the number of multiple comparisons. First, we calculated population means ($n_{\text{participants}} = 216$) for each region and each MRI modality, thus acquiring six inter-regional profiles across the 34 cortical regions. We then carried out PCA on the MRI inter-regional profiles to obtain the loadings of the first two leading components (PC1 and PC2) that have eigenvalue >1. The loadings were applied to individual-level MRI data to calculate PC scores (for PC1 and PC2) for each individual and each cortical region. Briefly, for each region, the original (MRI) values were scaled within each modality and then multiplied by their corresponding PC loadings. Then we summed the product of scaled values and PC loadings for each participant. Thus, we derived PC1 and PC2 "matrices" with 34 regions (and 216 individuals), and used the matrices for the following analyses.

Cortical Structure and Pubertal Testosterone

The distribution of APTC in our sample is bimodal (Supplementary Figure S2), with peaks at 153 and 174 months (Mean: 162.87, SD: 10.42). We observed a negative correlation between pubertal-T and APTC ($r = -0.589$, $P < 0.001$). To examine whether the timing of testosterone surge modulates the relationship between overall pubertal-T exposure and cerebral cortex, we tested the interaction between pubertal-T and APTC using the following linear interaction model: (PC1 (or PC2) $\sim$ pubertal-T+APTC+ pubertal-T$\times$APTC). All variables were scaled and age-corrected. For each PC matrix, beta-coefficient of the interaction term (i.e., pubertal-T $\times$ APTC) is generated for each of 34 regions, resulting in an inter-regional profile of beta values across the 34 regions (indicating the effect size of interaction effects). Subsequently, we tested significance of the interaction (beta) profiles across the 34 regions for each PC matrix using a permutation approach. Specifically, the permutation test included the following steps: 1) fitted the null model without interaction (PC1 (or PC2) $\sim$ pubertal-T + APTC) and obtained residuals for all 34 regions; 2) permuted puberal-T; and 3) fitted the interaction model with the permuted pubertal-T and obtained beta-coefficient for the interaction term for each of the 34 regions; 4) repeated steps 2) and 3) 5000 times, and then averaged the 5000 simulated profiles to derive a null profile; 5) used paired t-test to test if the observed beta profile was different from the null profile, and thus, obtained the significance level with correction for false discovery rate (FDR) for 2 PC matrices.

We observed that beta profiles of the interaction term (pubertal-T × APTC) were different from null profiles for both PC1 and PC2. To investigate details in the correlation between pubertal-T and brain structure and the modulation effect of timing of testosterone surge, we divided participants into two groups: Early surge (APTC < mean) and late surge (APTC > mean) groups (Supplementary Table 1) based on the mean of APTC (i.e., 162.87 months). Negative correlation between pubertal-T and APTC was found within each group (Early: $r = -0.326$, $P = 0.003$; late: $r = -0.264$, $P = 0.010$), indicating possible confounding effect of APTC in correlation between pubertal-T and brain structure. Therefore, within each group, we corrected for APTC and age using residuals from the linear model (pubertal-T/Cortical structure ~ age + APTC) to estimate corrected testosterone and cortical structure values (mean + residual). Subsequently, we calculated the correlation coefficients between (APTC- and age-corrected) pubertal-T and the two indices of cortical structure (i.e., PC1 and PC2 scores) for each of the 34 regions within each group. Thus, we obtained inter-regional profiles of correlation coefficients (PC1-T and PC2-T) for each of the two groups (early and late surge). Correlation coefficients were transformed with Fisher z-transformation before being used in the following analyses. To answer the question whether cortical structure is associated with pubertal-T, we used a permutation approach to test the significance of each correlation-coefficient profile, with correction for FDR for the number of groups and matrices. For each matrix, we 1) permuted pubertal-T and then 2) calculated correlation coefficients between the resampled pubertal-T and cortical variables to obtain a simulated correlation-coefficient profile; 3) repeated steps 1) and 2) 5000 times, and then averaged the 5000 simulated profiles to derive a null profile; 4) to test if the observed correlation-coefficient profile is different from the null profile, we compared the observed correlation-coefficient profile with the null profile using paired *t*-test, and obtained the significant level of the relationship between pubertal-T and cortical structure. To investigate details of how the age of testosterone surge moderates the relationship between pubertal-T and cortical structure, we tested group differences in correlation-coefficient profiles with paired *t*-test (matched inter-regional profiles). FDR for the 2 PC matrices was used to correct for multiple comparisons.

Virtual Histology

Using the method developed by French and Paus, gene expression from Allen Human Brain Atlas (Hawrylycz et al. 2012) were mapped to the 34 cortical regions segmented by FreeSurfer using the Desikan–Killiany atlas (French and Paus 2015). To ensure representativeness of the inter-regional profiles of gene expression across age and sex, we restricted the analysis to 2511 genes that had consistent inter-regional profiles of expression during childhood and adolescence as indicated by a two-stage consistency filter described by Shin et al (Shin et al. 2018). Next, four gene-panels related, respectively, to spine, dendrite, myelin, and axonal cytoskeleton/transport were created using genetic ontology (GO) terms and gene data from Allen Human Brain Atlas. Three out of the four panels were created using GO terms to capture genes associated with the spine, dendrite arbor, and myelin (Parker et al. 2020). The axon panel was created using GO terms to capture genes associated with axonal cytoskeleton and transport (Paus et al. 2014). Briefly, genes of mammals for each selected GO term were downloaded from AmiGO 2 database (August 2020), and then all gene symbols were converted to human genes using the R package "homologene" and, in turn, updated to current Entrez gene symbols using the "limma" package (Version 3.44.3). A total of 317, 984, 335, and 183 genes were identified as belonging to the spine, dendrite, myelin, and axon panels, respectively. These genes were then filtered for inclusion within the 2511 "consistent" genes. The following numbers of genes passed the filter and were retained for subsequent analyses: spine—78, dendrite—259, myelin—49, and axonal cytoskeleton/transport—44. Note that these panels are not exclusive. All 78 spine genes are included in the dendrite panel, 7 (3) myelin genes, 24 (9) axon genes overlapped with the dendrite (spine) genes, and 9 myelin genes overlapped with axon genes.

Our virtual histology approach was designed to test spatial (inter-regional) correlations between the variations in a phenotype of interest (in this case, strength of the relationship between pubertal-T and cortical structure) and inter-regional variations of gene expression across the same regions for each of the four gene panels. As done previously (Shin et al. 2018; Parker et al. 2020), each inter-regional correlation-coefficient profile was correlated with inter-regional expression profile of each gene from a given panel, and average correlation coefficient served as the test statistic. The significance of the test statistic for the panel was obtained with a resampling approach. Briefly, we selected randomly the same number of genes as in a given panel from the 2511 consistent genes and correlated the expression profile of these genes with the inter-regional correlation-coefficient profile. Then the average correlation coefficient of the sampled gene set was calculated. This was repeated for 10 000 iterations to generate the null distribution of average correlation coefficients. The test statistic (average correlation coefficient for the panel) was compared against the null distribution using a two-sided test with FDR for the four panels. All statistical analyses were done with R (version 4.0.1) with a significance threshold for *P*-values set at 0.05.

Results

Principal Component Analysis

PCA of the six MRI inter-regional profiles provided loadings of the first two leading components PC1 and PC2, which explained 51.38% and 19.32% of the variance (Fig. 1A), respectively. T1, T2, MWF, and FA metrics mainly contribute to PC1, with loadings 0.50, 0.49, −0.51, and 0.407, respectively (Fig. 1B). MTR and MD are main contributors to PC2 with loadings 0.80 and −0.51, respectively.

Brain Structure and Pubertal Testosterone

The beta profiles of the interaction term (pubertal-T × APTC) were different from null profiles in both PC matrices (PC1: $t = -5.53$, $P < 0.001$; PC2: $t = -2.77$, $P = 0.009$, Supplementary Figure S3). As shown in Figure 2, the inter-regional profiles of correlation coefficients quantifying the relationship between pubertal-T and PC1/PC2 (i.e., PC1-T and PC2-T) are positive in both early and late testosterone-surge groups ($P < 0.001$ for all correlation-coefficient profiles). Group comparison with paired *t*-test showed that the early surge group has stronger correlations between pubertal-T and cortical structure than the late surge group for both PCs (PC1-T: $P < 0.001$, df= 33, $t = 6.85$; PC2-T: $P < 0.001$, df= 33, $t = 8.87$). To facilitate understanding of these results, we also provide inter-regional profiles of correlation

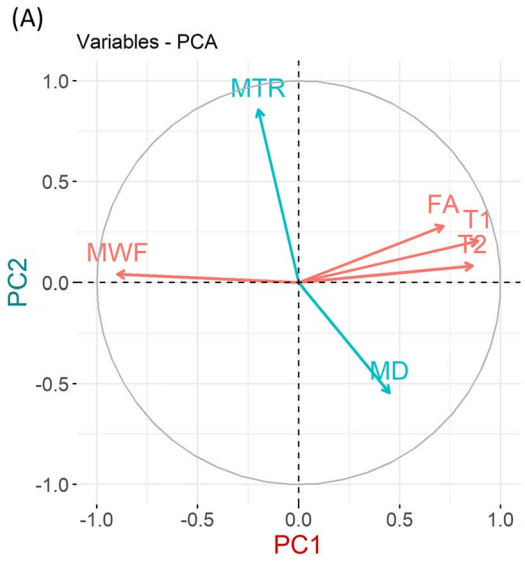

(B)

Modality	PC1	PC2
MWF	-0.511	0.038
T1	0.505	0.191
T2	0.489	0.076
FA	0.407	0.259
MTR	-0.114	0.795
MD	0.256	-0.506

Figure 1. PCA of the six MRI matrices. (A) Correlations between modalities and PC1 and PC2. The coordinates of a modality are correlations between the modality and PC1 (x coordinate) and PC2 (y coordinate). Modalities in red are the main contributors to PC1, and modalities in blue are the main contributors to PC2. (B) Loadings of the six MRI modalities on PC1 and PC2.

coefficients quantifying associations between pubertal-T and the six MRI metrics (Supplementary Figure S4). We observed a weak albeit significant correlation between pubertal testosterone and current (on the day of the MR scan) testosterone level ($r = 0.163$, $P = 0.017$). To evaluate the possible confounding effect of current testosterone on the relationship between pubertal testosterone and brain structure, we have carried out the additional analysis in which we controlled for the levels of current testosterone. The results remained virtually the same (see Supplementary Figure S5).

Virtual Histology

As shown in Figure 3 and Table 1, the associations between interregional correlation-coefficient profiles and gene-expression profiles of the four panels varied across MRI metrics (PC1, PC2) and groups (early, late surge). The PC1-T profile is positively correlated with myelin and axon panels in the early surge group only (Table 1). Nominal associations between PC2-T and spine and dendrite panels were observed in the early and late surge group, respectively, but the associations did not survive FDR correction (Table 1).

Discussion

In this study, we found that the level of pubertal testosterone correlates with structural properties of cerebral cortex in young men. Timing of a testosterone surge modulates this relationship; earlier peak of change in testosterone levels predicts a stronger association between pubertal testosterone and brain structure, as compared with a peak occurring (on average) 20 months later. The latter observation suggests that the decreasing window of sensitivity to testosterone throughout adolescence found in rodent (behavioral) studies may also exist in humans. Furthermore, our results of virtual histology suggest that the relationship between pubertal-T and cerebral cortex may be related to cellular processes involving axonal cytoskeleton and transport, myelin, and dendritic arbor.

The results of pubertal-T and PC1 point to possible organizational effects of testosterone on axonal cytoskeleton and transport, and myelination. The MRI modalities captured by PC1, namely MWF, T1, T2, and FA are believed to be sensitive to myelin and water content (Laule et al. 2007, 2008; Edwards et al. 2018). Thus, the observed positive correlation between pubertal-T and PC1 appears to suggest that higher pubertal-T during early puberty is associated with lower myelin and higher water content in the cerebral cortex. When myelin is considered in absolute terms, this observation appears in conflict with findings from animal studies consistent with androgens-related increases in the density of oligodendrocytes and, in turn, myelination in the rat corpus callosum (Patel et al. 2013; Abi Ghanem et al. 2017). Our exploratory analysis (Supplementary Figure S4) showed that there is a positive relationship between T1 relaxation time and pubertal-T but no association between MWF and pubertal-T. The present results of virtual histology are consistent with a process by which testosterone facilitates the radial growth of (intracortical) axons, diluting—in turn—myelin content in the imaged sample of tissue (voxel). Such a testosterone-related axon-myelin shift is reflected in *g* ratio (defined as axon diameter/fiber diameter; where fiber diameter = axon diameter + myelin sheath); in rats, we have observed a higher *g* ratio in the corpus callosum in males versus females, and a lower g ratio in castrated versus intact males (Pesaresi et al. 2015). Altogether, we suggest that the observed relationship between pubertal-T and PC1 fits best a model that takes into account competing influences of axonal and myelin compartments, respectively, on the relevant MR signals. In this scenario, as the axon diameter increases, the relative amount of myelin decreases; as pointed out above, even if there is an absolute increase in myelination, thicker axons have relatively thinner myelin sheath (Paus and Toro 2009). Thus, compared with the cerebral cortex of individuals with lower pubertal-T, the cortex of individuals with

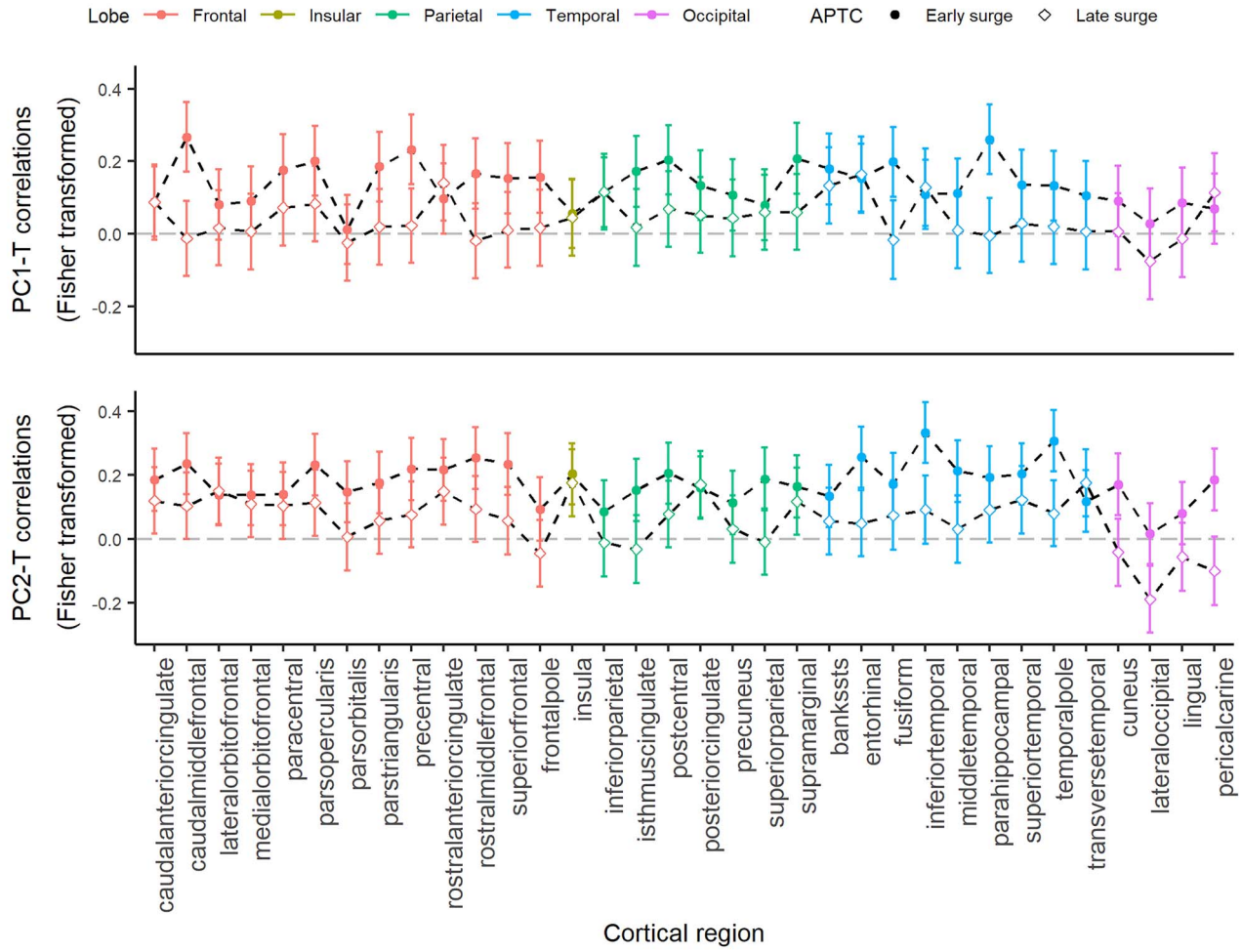

Figure 2. Inter-regional profiles of Fisher-transformed correlation coefficient between pubertal testosterone and brain cortex variables PC1 and PC2 in the early and late surge group. Dashed lines with solid circles represent profiles of the early surge group, dashed lines with the empty square are profiles of the late surge group. Error bar represents ±1 SD of correlation coefficients.

Table 1 Results of virtual histology with gene panels

Profile	Panels	Average *r*	P	p.adj (FDR)
early PC1-T	Myelin	0.061	0.019*	0.041**
	Dendrite	0.008	0.334	0.388
	Spine	0.016	0.388	0.388
	Axon	0.066	0.020*	0.041**
late PC1-T	Myelin	0.018	0.811	0.811
	Dendrite	0.009	0.806	0.811
	Spine	0.026	0.462	0.811
	Axon	-0.006	0.533	0.811
early PC2-T	Myelin	0.024	0.800	0.800
	Dendrite	0.043	0.128	0.255
	Spine	0.100	0.023*	0.092
	Axon	-0.008	0.712	0.800
late PC2-T	Myelin	0.049	0.538	0.717
	Dendrite	0.066	0.032*	0.123
	Spine	0.100	0.062	0.123
	Axon	0.017	0.938	0.938

Note: Average correlation coefficients were obtained by correlating inter-regional profiles of correlation between pubertal-T and cerebral cortex to expression profiles of genes in gene panels. * P-value < 0.05 (nominal). ** P-value < 0.05 (FDR corrected).

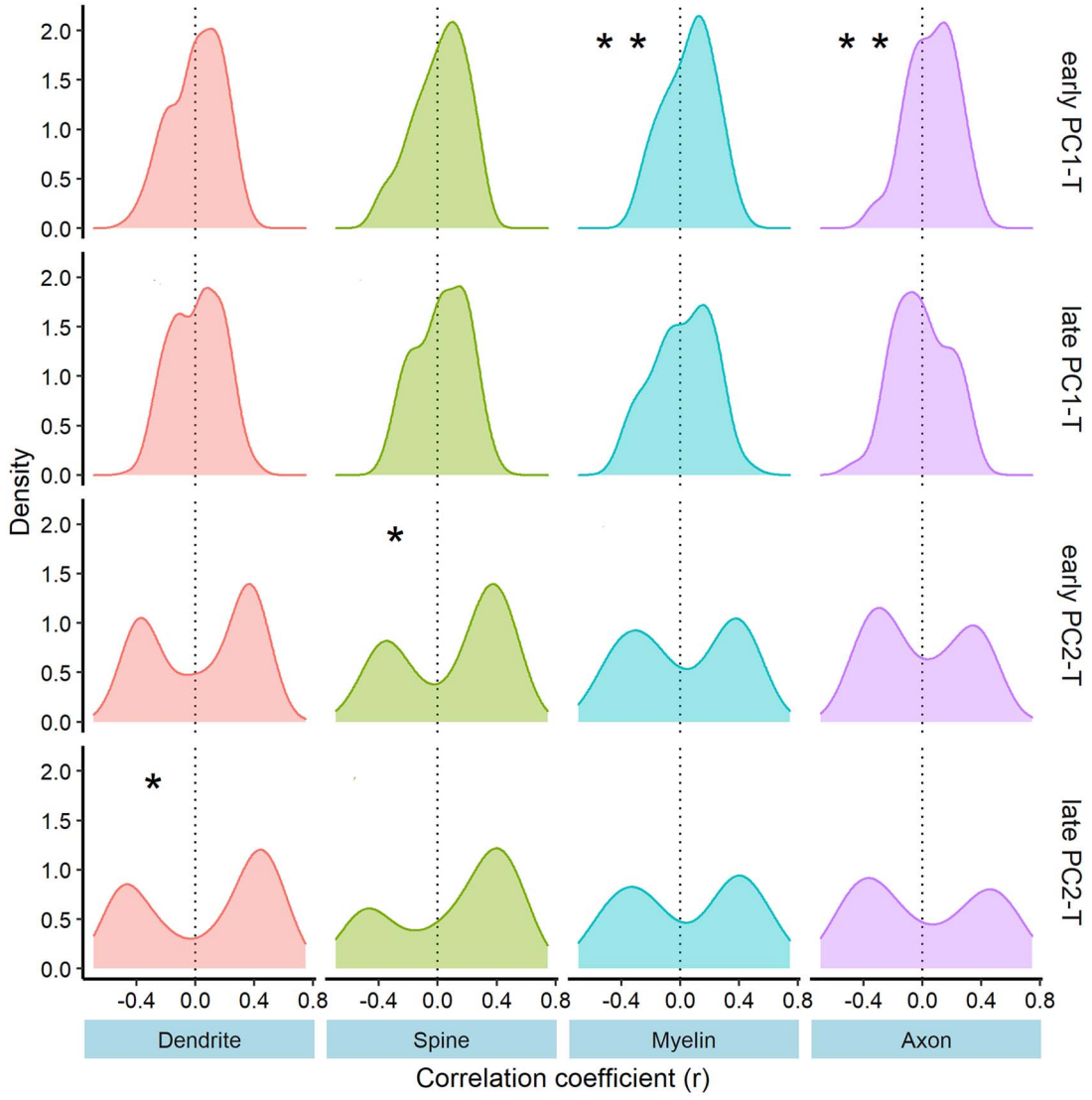

Figure 3. Distribution of Pearson correlation coefficients between inter-regional correlation-coefficient profiles and inter-regional expression of genes in the four panels. Significance of mean correlation coefficient from the null distribution is calculated using a resampling technique. ∗P-value < 0.05; ∗∗FDR (correcting for four panels) $P < 0.05$.

higher pubertal testosterone appears more "gray" (longer T1 relaxation times). Overall, we suggest that the observed association between a higher pubertal-T and the higher PC1 values may indicate relatively thicker axons with relatively thinner myelin sheaths.

The results of PC2 and pubertal-T indicate the relationship between testosterone and dendritic arbor and spines. Note, however, that these relationships are not as robust as those observed for PC1 with regards to myelin and axons (described above). The PC2 is primarily loaded by MTR (positively) and MD (negatively). MTR is sensitive to macromolecules. In the human cerebral cortex, our previous work suggests that MTR in the cortex varies mainly as a function of the extent of cellular membranes (owing to their macromolecular composition) constituting the extensive dendritic arbor of pyramidal neurons of the human cerebral cortex (Patel et al. 2019). MTR depends on the transfer of spins between bound (large molecules) and free (water) protons. There is a disproportional amount of surface area associated with myelin sheaths (~48 m^2), dendrite, and spine (~980 m^2) in cerebral cortex (see detailed hypothetical estimation in Patel et al. 2019). The bound pool of protons consists of hydrogen nuclei bound to semi-solid macromolecular structures, such as large macromolecules and cellular membranes. Given this, it is likely that greater amount of neurites (dendrites and spines) may lead to higher number of bound protons and, in turn, higher MTR. Thus, the positive correlation between pubertal-T and PC2 suggests that higher pubertal-T is related to a more extensive dendritic arbor. This is partially supported by our results of the positive association between PC2-T correlation-coefficient profiles and the inter-regional expression profiles of genes in the dendrite panel. These findings are consistent with results of previous experimental studies that showed the effects of testosterone on growth and maintenance of dendrites in rats' hippocampus and cell cultures (Leranth et al. 2003; Fargo et al.

2008; Hatanaka et al. 2009). For example, gonadectomy led to an almost 50% reduction (compared with intact males) in the density of spine synapse on pyramidal neurons (Leranth et al. 2003).

The significant interaction beta-coefficients (pubertal-T and age of testosterone surge) profiles and the differences between the early and late surge groups in the strength of correlation between pubertal-T and cortical structure suggest that there is a decreasing window of sensitivity to testosterone throughout adolescence in human. Since the time of testosterone surge of both early and late groups was within the normal pubertal timing (Palmert and Boepple 2001), and the mean differences in the APTC between the two groups are about 20 months, it is unlikely that there is a sensitive window that opens at the onset of puberty, with the surge of testosterone of the late group being out of this window. In fact, the influence of testosterone on brain structure can extend into adulthood as shown in both animal (Hatanaka et al. 2009) and human studies (Azad et al. 2003; Pol et al. 2006). Thus, our results suggest that the organizational effects of testosterone on brain structure might decrease gradually throughout adolescence. Mechanisms of such age-related differences in sensitivity to organizational effects of testosterone are unknown. Due to the complexity of downstream regulation of testosterone (Fargo et al. 2016), there are several possibilities. One scenario would involve genomic and/or transcriptomic variations in key molecules initiating nuclear effects of testosterone, such as androgen receptor (AR). For instance, genetic polymorphisms in AR can lead to varied strength of associations between testosterone and brain structure (Paus et al. 2010). In terms of AR expression, a few studies in mice suggest, however, that its expression increases rather than decreases with age in the developing cerebral cortex and hippocampus (Nuñez et al. 2003; Tsai et al. 2015). On the other hand, with evidence of up-regulation of AR expression by androgens in rodent studies (Takeda et al. 1991; Kerr et al. 1995), early exposure to testosterone may lead to higher expression of AR in the brain and ultimately, a higher sensitivity to testosterone. The other possibility is that testosterone may moderate the efficiency of mediators, such as brain-derived neurotrophic factor (BDNF), that are essential for brain plasticity. As the levels of these factors change, the strength of an association between testosterone and brain structure changes as well. For example, testosterone is known to regulate the effect of BDNF dendritic morphology of spinal motoneurons; absence of either BDNF or testosterone leads to lower dendritic length and density, as compared with a control group with both BDNF and testosterone on board (Yang et al. 2004). An age-related decrease in levels of BDNF level was found in human and rats studies (Katoh-Semba et al. 1998; Yatham et al. 2009); this might contribute to a weak correlation between testosterone and brain structure in individuals with late testosterone surge.

Limitations

There are several limitations to consider in this study. First, it is important to note that the participants are males only. This may limit generalizability of our findings as some studies showed sex differences in testosterone-related brain maturation (Bramen et al. 2012; Parker et al. 2017). Second, we used gene-expression data obtained from six postmortem adult brains in the Allen Human Brain Atlas. Although limited in the number of donors, this atlas provides the most comprehensive coverage of gene expression across the entire (human) cerebral cortex. To maximize representativeness of the inter-regional profiles, we applied the two-stage consistency filter to genes related to selected GO terms and restricted our analysis to genes with statistically consistent inter-regional profiles of expression from childhood to adulthood (and males and females). Note that the results are from the left hemisphere and some studies showed hemispheric differences in testosterone-related brain maturation (Pfannkuche et al. 2009; Nguyen et al. 2013), this may limit generalizability of the results to the right hemisphere. Nevertheless, we observed very strong correlations between inter-regional profiles of the six MR modalities obtained in the left and right hemispheres, respectively. Finally, the lack of longitudinal MRI data does not allow us to determine when the observed testosterone-related variations in structural properties of the cerebral cortex emerged or might disappear. On the other hand, detailed testosterone trajectories (five longitudinal samples in each participant) provide robust estimates of the hormonal milieu in which an individual's brain matured during puberty. Future longitudinal studies with testosterone and MRI collected in parallel throughout adolescence would provide missing details with regards to the role of pubertal testosterone in shaping brain structure during this developmental period.

Conclusion

The primary aim of the present study was to investigate the relationship between pubertal testosterone and structure of the human cerebral cortex, and possible modulation of this relationship by the timing of testosterone surge during puberty. We have found that—in young men—the level of pubertal testosterone correlates with structural properties of cerebral cortex. This relationship is modulated by timing of testosterone surge: earlier peak of change in testosterone levels predicts a stronger relationship. These observations provide evidence supporting the Schulz and Sisk model, namely that of postnatal decrease in organizational effects of gonadal steroid hormones (Schulz and Sisk 2016). Considering the limitations of this study, more work needs to be done to examine more closely existence of the decreasing window of sensitivity to sex hormone throughout adolescence in humans, in particular extending our finding to females and estrogen. This work also offers initial insights into the neurobiology underlying the association between pubertal-T and structure of cortical regions, suggesting that it may be related to cellular processes involving axonal cytoskeleton and myelin, and—possibly—also dendritic arbor.

Supplementary Material

Supplementary material can be found at *Cerebral Cortex* online.

Notes

We are extremely grateful to all the families who took part in this study the whole ALSPAC team, which includes midwives, interviewers, computer and laboratory technicians, clerical workers, research scientists, volunteers, managers, receptionists, and nurses. *Conflict of interest*: None declared.

Funding

The UK Medical Research Council and Wellcome (Grant ref: 102215/2/13/2) and the University of Bristol provide core support

for ALSPAC. A comprehensive list of grants funding is available on the ALSPAC website (http://www.bristol.ac.uk/alspac/external/documents/grant-acknowledgements.pdf). This research was specifically funded by Wellcome Trust and Medical Research Council (076467/Z/05/Z). This research was supported by a grant from the National Institutes of Health (R01MH085772 to T.P.). This publication is the work of the authors and T.P. will serve as guarantors for the contents of this paper, and it does not necessarily represent the official views of the National Institutes of Health. Z.L. is supported by Chinese Scholarship Grant (201806380177).

References

Abi Ghanem C, Degerny C, Hussain R, Liere P, Pianos A, Tourpin S, Habert R, Macklin WB, Schumacher M, Ghoumari AM. 2017. Long-lasting masculinizing effects of postnatal androgens on myelin governed by the brain androgen receptor. *PLoS Genet*. 13:1–26.

Avants B, Tustison N, Song G. 2009. Advanced normalization tools (ANTS). *Insight J*. 2:1–35.

Azad N, Pitale S, Barnes WE, Friedman N. 2003. Testosterone treatment enhances regional brain perfusion in hypogonadal men. *J Clin Endocrinol Metab*. 88:3064–3068.

Björnholm L, Nikkinen J, Kiviniemi V, Nordström T, Niemelä S, Drakesmith M, Evans JC, Pike GB, Veijola J, Paus T. 2017. Structural properties of the human corpus callosum: multimodal assessment and sex differences. *Neuroimage*. 152:108–118.

Boyd A, Golding J, Macleod J, Lawlor DA, Fraser A, Henderson J, Molloy L, Ness A, Ring S, Smith GD. 2013. Cohort profile: the 'children of the 90s'-the index offspring of the Avon longitudinal study of parents and children. *Int J Epidemiol*. 42:111–127.

Bramen JE, Hranilovich JA, Dahl RE, Chen J, Rosso C, Forbes EE, Dinov ID, Worthman CM, Sowell ER. 2012. Sex matters during adolescence: testosterone-related cortical thickness maturation differs between boys and girls. *PLoS One*. 7:1–9.

Coniglio LP, Clemens LG. 1976. Period of maximal susceptibility to behavioral modification by testosterone in the golden hamster. *Horm Behav*. 7:267–282.

Deoni SCL, Rutt BK, Arun T, Pierpaoli C, Jones DK. 2008. Gleaning multicomponent T 1 and T 2 information from steady-state imaging data. *Magn Reson Med*. 60:1372–1387.

Desikan RS, Ségonne F, Fischl B, Quinn BT, Dickerson BC, Blacker D, Buckner RL, Dale AM, Maguire RP, Hyman BT et al. 2006. An automated labeling system for subdividing the human cerebral cortex on MRI scans into gyral based regions of interest. *Neuroimage*. 31:968–980.

Eaton G. 1970. Effect of a single Prepubertal injection of testosterone propionate on adult bisexual behavior of male hamsters castrated at birth 1. *Endocrinology*. 87:934–940.

Edwards LJ, Kirilina E, Mohammadi S, Weiskopf N. 2018. Microstructural imaging of human neocortex in vivo. *Neuroimage*. 182:184–206.

Fargo KN, Galbiati M, Foecking EM, Poletti A, Jones KJ. 2008. Androgen regulation of axon growth and neurite extension in motoneurons. *Horm Behav*. 53:716–728.

Fargo KN, Pak TR, Foecking EM, Jon KJ. 2016. Molecular Biology of Androgen Action: Perspectives on Neuroprotective and Neurotherapeutic Effects. In: Pfaff DW„ Joels M, editors. *Hormones, Brain and Behavior*. 3rd ed. Cambridge, MA: Academic Press Inc. pp. 1219–1239.

Fraser A, Macdonald-wallis C, Tilling K, Boyd A, Golding J, Davey Smith G, Henderson J, Macleod J, Molloy L, Ness A et al. 2013. Cohort profile: The Avon longitudinal study of parents and children: ALSPAC mothers cohort. *Int J Epidemiol*. 42:97–110.

French L, Paus T. 2015. A FreeSurfer view of the cortical transcriptome generated from the Allen human brain atlas. *Front Neurosci*. 9:323.

Goldstein LA, Kurz EM, Sengelaub DR. 1990. Androgen regulation of dendritic growth and retraction in the development of a sexually dimorphic spinal nucleus. *J Neurosci*. 10:935–946.

Hatanaka Y, Mukai H, Mitsuhashi K, Hojo Y, Murakami G, Komatsuzaki Y, Sato R, Kawato S. 2009. Androgen rapidly increases dendritic thorns of CA3 neurons in male rat hippocampus. *Biochem Biophys Res Commun*. 381:728–732.

Hawrylycz MJ, Lein ES, Guillozet-Bongaarts AL, Shen EH, Ng L, Miller JA, van de Lagemaat LN, Smith KA, Ebbert A, Riley ZL et al. 2012. An anatomically comprehensive atlas of the adult human brain transcriptome. *Nature*. 489:391–399.

Herting MM, Gautam P, Spielberg JM, Kan E, Dahl RE, Sowell ER. 2014. The role of testosterone and estradiol in brain volume changes across adolescence: a longitudinal structural MRI study. *Hum Brain Mapp*. 35:5633–5645.

Jenkinson M, Beckmann CF, Behrens TE, Woolrich MW, Smith SM. 2012. FSL 1. *Neuroimage*. 62:782–790.

Jensen SKG, Pangelinan M, Björnholm L, Klasnja A, Leemans A, Drakesmith M, Evans CJ, Barker ED, Paus T. 2018. Associations between prenatal, childhood, and adolescent stress and variations in white-matter properties in young men. *Neuroimage*. 182:389–397.

Katoh-Semba R, Semba R, Takeuchi IK, Kato K. 1998. Age-related changes in levels of brain-derived neurotrophic factor in selected brain regions of rats, normal mice and senescence-accelerated mice: a comparison to those of nerve growth factor and neurotrophin-3. *Neurosci Res*. 31:227–234.

Kerr JE, Allore RJ, Beck SG, Handa RJ. 1995. Distribution and hormonal regulation of androgen receptor (ar) and ar messenger ribonucleic acid in the rat hippocampus. *Endocrinology*. 136:3213–3221.

Khairullah A, Klein LC, Ingle SM, May MT, Whetzel CA, Susman EJ, Paus T. 2014. Testosterone trajectories and reference ranges in a large longitudinal sample of male adolescents. *PLoS One*. 9:e108838.

Laule C, Kozlowski P, Leung E, Li DKB, MacKay AL, Moore GRW. 2008. Myelin water imaging of multiple sclerosis at 7 T: correlations with histopathology. *Neuroimage*. 40:1575–1580.

Laule C, Vavasour IM, Kolind SH, Li DKB, Traboulsee TL, Moore GRW, MacKay AL. 2007. Magnetic resonance imaging of myelin. *Neurotherapeutics*. 4:460–484.

Leranth C, Petnehazy O, MacLusky NJ. 2003. Gonadal hormones affect spine synaptic density in the CA1 hippocampal subfield of male rats. *J Neurosci*. 23:1588–1592.

Mack CM, Boehm GW, Berrebi AS, Denenberg VH. 1995. Sex differences in the distribution of axon types within the genu of the rat corpus callosum. *Brain Res*. 697:152–156.

Mancini M, Karakuzu A, Cohen-Adad J, Cercignani M, Nichols TE, Stikov N. 2020. An interactive meta-analysis of MRI biomarkers of myelin. *Elife*. 9:e61523, 1–23.

Neufang S, Specht K, Hausmann M, Güntürkün O, Herpertz-Dahlmann B, Fink GR, Konrad K. 2009. Sex differences and the impact of steroid hormones on the developing human brain. *Cereb Cortex*. 19:464–473.

Nguyen TV, McCracken J, Ducharme S, Botteron KN, Mahabir M, Johnson W, Israel M, Evans AC, Karama S. 2013. Testosterone-related cortical maturation across childhood and adolescence. *Cereb Cortex*. 23:1424–1432.

Nguyen TV. 2018. Developmental effects of androgens in the human brain. *J Neuroendocrinol*. 30:1–13.

Nuñez JL, Huppenbauer CB, McAbee MD, Juraska JM, DonCarlos LL. 2003. Androgen receptor expression in the developing male and female rat visual and prefrontal cortex. *J Neurobiol*. 56:293–302.

O'Muircheartaigh J, Vavasour I, Ljungberg E, Li DKB, Rauscher A, Levesque V, Garren H, Clayton D, Tam R, Traboulsee A et al. 2019. Quantitative neuroimaging measures of myelin in the healthy brain and in multiple sclerosis. *Hum Brain Mapp*. 40:2104–2116.

Palmert MR, Boepple PA. 2001. Variation in the timing of puberty: clinical spectrum and genetic investigation. *J Clin Endocrinol Metab*. 86:2364–2368.

Parker N, Parker N, Patel Y, Patel Y, Jackowski AP, Jackowski AP, Pan PM, Salum GA, Salum GA, Pausova Z et al. 2020. Assessment of neurobiological mechanisms of cortical thinning during childhood and adolescence and their implications for psychiatric disorders. *JAMA Psychiat*. 1–10.

Parker N, Wong APY, Leonard G, Perron M, Pike B, Richer L, Veillette S, Pausova Z, Paus T. 2017. Income inequality, gene expression, and brain maturation during adolescence. *Sci Rep*. 7:7397.

Patel R, Moore S, Crawford DK, Hannsun G, Sasidhar MV, Tan K, Molaie D, Tiwari-Woodruff SK. 2013. Attenuation of corpus callosum axon myelination and remyelination in the absence of circulating sex hormones. *Brain Pathol*. 23:462–475.

Patel Y, Shin J, Drakesmith M, Evans J, Pausova Z, Paus T. 2020. Virtual histology of multi-modal magnetic resonance imaging of cerebral cortex in young men. *Neuroimage*. 218:116968.

Patel Y, Shin J, Gowland PA, Pausova Z, Paus T. 2019. Maturation of the human cerebral cortex during adolescence: myelin or dendritic arbor? *Cereb Cortex*. 29:3351–3362.

Paus T, Nawaz-Khan I, Leonard G, Perron M, Pike GB, Pitiot A, Richer L, Susman E, Veillette S, Pausova Z. 2010. Sexual dimorphism in the adolescent brain: role of testosterone and androgen receptor in global and local volumes of grey and white matter. *Horm Behav*. 57:63–75.

Paus T, Pesaresi M, French L. 2014. White matter as a transport system. *Neuroscience*. 276:117–125.

Paus T, Toro R. 2009. Could sex differences in white matter be explained by g ratio? *Front Neuroanat*. 3:1–7.

Peper JS, Brouwer RM, Schnack HG, van Baal GC, van Leeuwen M, van den Berg SM, Delemarre-Van de Waal HA, Boomsma DI, Kahn RS, Hulshoff Pol HE. 2009. Sex steroids and brain structure in pubertal boys and girls. *Psychoneuroendocrinology*. 34:332–342.

Peper JS, Hulshoff Pol HE, Crone EA, van Honk J. 2011. Sex steroids and brain structure in pubertal boys and girls: a mini-review of neuroimaging studies. *Neuroscience*. 191:28–37.

Perrin JS, Hervé PY, Leonard G, Perron M, Pike GB, Pitiot A, Richer L, Veillette S, Pausova Z, Paus T. 2008. Growth of white matter in the adolescent brain: role of testosterone and androgen receptor. *J Neurosci*. 28:9519–9524.

Pesaresi M, Soon-Shiong R, French L, Kaplan DR, Miller FD, Paus T. 2015. Axon diameter and axonal transport: in vivo and in vitro effects of androgens. *Neuroimage*. 115:191–201.

Pfaff DW, Joëls M. 2016. *Hormones, Brain and Behavior*. Cambridge, MA: Academic Press Inc.

Pfannkuche KA, Bouma A, Groothuis TGG. 2009. Does testosterone affect lateralization of brain and behaviour? A meta-analysis in humans and other animal species. *Philos Trans R Soc B Biol Sci*. 364:929–942.

Phoenix CH, Goy RW, Gerall AA, Young WC. 1959. Organizing action of prenatally administered testosterone propionate on the tissues mediating mating behavior in the female Guinea pig. *Endocrinology*. 65:369–382.

Pol HEH, Cohen-Kettenis PT, Van Haren NEM, Peper JS, Brans RGH, Cahn W, Schnack HG, Gooren LJG, Kahn RS. 2006. Changing your sex changes your brain: influences of testosterone and estrogen on adult human brain structure. *Eur J Endocrinol*. 155:S107–S114.

Schulz KM, Molenda-Figueira HA, Sisk CL. 2009a. Back to the future: the organizational-activational hypothesis adapted to puberty and adolescence. *Horm Behav*. 55:597–604.

Schulz KM, Sisk CL. 2006. Pubertal hormones, the adolescent brain, and the maturation of social behaviors: lessons from the Syrian hamster. *Mol Cell Endocrinol*. 254–255:120–126.

Schulz KM, Sisk CL. 2016. The organizing actions of adolescent gonadal steroid hormones on brain and behavioral development. *Neurosci Biobehav Rev*. 70:148–158.

Schulz KM, Zehr JL, Salas-Ramirez KY, Sisk CL. 2009b. Testosterone programs adult social behavior before and during, but not after, adolescence. *Endocrinology*. 150:3690–3698.

Shin J, French L, Xu T, Leonard G, Perron M, Pike GB, Richer L, Veillette S, Pausova Z, Paus T. 2018. Cell-specific gene-expression profiles and cortical thickness in the human brain. *Cereb Cortex*. 28:3267–3277.

Sisk CL, Zehr JL. 2005. Pubertal hormones organize the adolescent brain and behavior. *Front Neuroendocrinol*. 26:163–174.

Södergard R, Bäckström T, Shanbhag V, Carstensen H. 1982. Calculation of free and bound fractions of testosterone and estradiol-17β to human plasma proteins at body temperature. *J Steroid Biochem*. 16:801–810.

Takeda H, Nakamoto T, Kokontis J, Chodak GW, Chang C. 1991. Autoregulation of androgen receptor expression in rodent prostate: Immunohistochemical and in situ hybridization analysis. *Biochem Biophys Res Commun*. 177: 488–496.

Tofts P. 2003. *Quantitative MRI of the brain: measuring changes caused by disease*. Chichester (UK): John Wiley and Sons Ltd.

Tsai H-W, Taniguchi S, Samoza J, Ridder A. 2015. Age- and sex-dependent changes in androgen receptor expression in the developing mouse cortex and hippocampus. *Neurosci J*. 2015:1–11.

Uematsu H, Popescu A, Zhang G, Wright AC, Wehrli SL, Takahashi M, Wehrli FW, Selzer ME, Hackney DB. 2004. Magnetization transfer micro-MR imaging of live excised lamprey spinal cord: characterization and immunohistochemical correlation. *Am J Neuroradiol*. 25:1816–1820.

Yang LY, Verhovshek T, Sengelaub DR. 2004. Brain-derived neurotrophic factor and androgen interact in the maintenance of dendritic morphology in a sexually dimorphic rat spinal nucleus. *Endocrinology*. 145:161–168.

Yatham LN, Kapczinski F, Andreazza AC, Trevor Young L, Lam RW, Kauer-Sant'Anna M. 2009. Accelerated age-related decrease in brain-derived neurotrophic factor levels in bipolar disorder. *Int J Neuropsychopharmacol*. 12:137.